Hypercholesterolemia impairs collateral artery enlargement by ten-eleven translocation 1-dependent hematopoietic stem cell autonomous mechanism in a murine model of limb ischemia

Jinglian Yan, PhD, Guodong Tie, PhD, Amanda Tutto, MS, *and* Louis M. Messina, MD, *Worcester, MA*

ABSTRACT

Objective: The extent of collateral artery enlargement determines the risk of limb loss due to peripheral arterial disease. Hypercholesterolemia impairs collateral artery enlargement, but the underlying mechanism remains poorly characterized. This study tests the hypothesis that hypercholesterolemia impairs collateral artery enlargement through a ten-eleven translocation 1 (Tet1)-dependent hematopoietic stem cell (HSC)-autonomous mechanism that increases their differentiation into proinflammatory Ly6C^{hi} monocytes and restricts their conversion into proangiogenic Ly6C^{low} monocytes.

Methods: To test our hypothesis, we induced limb ischemia and generated chimeric mouse models by transplanting HSCs from either wild-type (WT) mice or hypercholesterolemic mice into lethally irradiated WT recipient mice.

Results: We found that the lethally irradiated WT recipient mice reconstituted with HSCs from hypercholesterolemic mice displayed lower blood flow recovery and collateral artery enlargement that was nearly identical to that observed in hypercholesterolemic mice, despite the absence of hypercholesterolemia and consistent with an HSC-autonomous mechanism. We showed that hypercholesterolemia impairs collateral artery enlargement by a Tet1-dependent mechanism that increases HSC differentiation toward proinflammatory Ly6C^{hi} monocytes and restricts the conversion of Ly6C^{hi} monocytes into proangiogenic Ly6C^{low} monocytes. Moreover, Tet1 epigenetically reprograms monocyte gene expression within the HSCs. Restoration of Tet1 expression in HSCs of hypercholesterolemic mice restores WT collateral artery enlargement and blood flow recovery after induction of hindlimb ischemia.

Conclusions: These results show that hypercholesterolemia impairs collateral artery enlargement by a novel Tet1-dependent HSC-autonomous mechanism that epigenetically reprograms monocyte gene expression within the HSCs. (JVS—Vascular Science 2024;5:100203.)

Clinical Relevance: The extent of collateral artery enlargement determines the risk of limb loss due to peripheral arterial occlusive disease, survival after acute myocardial infarction, and the occurrence of neurological deficits after ischemic stroke. Yet, the mechanisms that regulate collateral artery enlargement are incompletely characterized. We show that hypercholesterolemia impairs collateral artery enlargement by a hematopoietic stem cell (HSC)-autonomous mechanism where the monocyte number and gene expression are epigenetically reprogrammed within the HSC. Thus, therapeutic agents for peripheral arterial disease should focus on normalizing the immune response during collateral artery enlargement.

Keywords: Collateral artery; Hematopoietic stem cells; Epigenetics; Hypercholesterolemia; Monocytes; Peripheral vascular disease

The principal physiological response to arterial occlusion is collateral artery enlargement, a form of arteriogenesis that is the key component of postischemic neovascularization.[1,2] The extent of collateral artery enlargement determines the risk of limb loss due to peripheral arterial occlusive disease, survival after acute myocardial infarction, and the extent of neurological deficits after ischemic stroke.

Collateral arteries are present at birth, and their number and diameter are determined genetically.[3] Collateral arteries have little or no blood flow until an arterial occlusion creates a pressure gradient that initiates blood

---

flow through the collateral arteries. This increased blood flow through the collateral arteries increases tangential fluid shear stress, which activates endothelial cells. The activated endothelial cells trigger postischemic neovascularization, inducing the expression of cell adhesion molecules, which attracts inflammatory cells and their subsequent diapedesis into the extracellular matrix to promote collateral artery enlargement through matrix degradation and the secretion of multiple cytokines.[4]

Monocytes are widely recognized as the pivotable inflammatory cell during collateral artery enlargement. A direct correlation between the number of circulating monocytes and collateral artery enlargement has been well established in preclinical and clinical studies.[5-11] Monocytes include two functionally distinct subsets in mice: Ly6C^{hi} and Ly6C^{low} subsets, corresponding to the CD14^{+}CD16^{−} and CD14^{low}CD16^{+} subsets, respectively, in humans.[12] Based on their function and gene expression, Ly6C^{hi} monocytes are identified as classic monocytes or as the proinflammatory subset that initiates the inflammatory response induced by ischemic injury.[13] Generally, Ly6C^{low} monocytes, identified as a nonclassic or proangiogenetic subset, patrol along the luminal endothelial surface to monitor blood vessels and scavenge microparticles.[5] However, the mechanism regulating the number of circulating monocytes and their function during collateral artery enlargement remains incompletely characterized.

In response to an ischemic injury, extravasated Ly6C^{hi} monocytes and their terminal progeny can be found in almost all body tissues, contributing to the local tissue-resident macrophage pools.[14] An alternative maturation route for Ly6C^{hi} monocytes, rather than leaving the circulation to develop into tissue-specific monocyte-derived cells or to join the monocyte reservoirs, is their conversion into Ly6C^{low} monocytes.[15-17] The mechanisms that guide the conversion from Ly6C^{hi} monocytes into Ly6C^{low} monocytes are context specific.[18-20] Avraham-Davidi et al[19] showed that Ly6C^{hi} monocytes that were recruited into injured tissue underwent multiple phenotypic and functional changes, endowing them with enhanced proangiogenic capabilities and, importantly, with a markedly increased capacity to remodel existing small vessels into larger conduits, similar to what occurs during collateral artery enlargement.[19] Recent epigenetic experiments implied that DNA methylation and histone modifications also play a critical role in the maturation of monocytes.[20] However, it remains unknown whether cell-intrinsic mechanisms, especially epigenetic enzymes, are involved in the conversion from Ly6C^{hi} monocytes toward Ly6C^{low} monocytes. Moreover, each specific monocyte subset's precise role in collateral artery enlargement during postischemic neovascularization remains incompletely characterized.

Hypercholesterolemia causes a 10-fold higher risk of peripheral arterial disease and is also known to impair

ARTICLE HIGHLIGHTS

- **Type of Research:** A mouse model in vivo study
- **Key Findings:** Hypercholesterolemia impairs collateral artery enlargement by a ten-eleven translocation 1 (Tet1)-dependent hematopoietic stem cell-autonomous mechanism. Hypercholesterolemia downregulates Tet1, which increases proinflammatory Ly6C^{hi} monocytes and restricts their conversion into proangiogenic Ly6C^{low} monocytes. The dominant mechanism regulating collateral arteries, that are present since birth, is hematopoietic stem cell-derived monocyte subsets.
- **Take Home Message:** Hypercholesterolemia impairs collateral artery enlargement by a Tet1 hematopoietic stem cell-autonomous mechanism.

collateral artery enlargement, increasing the risk of limb loss.[21-26] Hypercholesterolemia impairs arteriogenesis by reducing the number of circulating monocytes.[27] Despite their substantial clinical importance, the specific mechanism by which hypercholesterolemia reduces circulating monocytes that impair collateral artery enlargement remains incompletely characterized. Recently, we have shown that hypercholesterolemia increases the incidence and pathologic severity of colorectal neoplasia by a hematopoietic stem cell (HSC)-autonomous mechanism.[28] Hypercholesterolemia induced an oxidized low-density lipoprotein (LDL)-dependent increase in HSC oxidant stress that downregulated Tet1 expression, resulting in reduced expression of genes critical to HSC production of natural killer T (NKT) and γδ T cells. These effects reduced the number and cytotoxicity of NKT and γδ T cells, impairing colorectal tumor immunosurveillance. This reduction in cytotoxicity unmasked a novel mechanism regulating immune cell gene expression: the effect of hypercholesterolemia was not due to a direct effect of hypercholesterolemia on the NKT and γδ T cell number and gene expression. Rather, these changes were mediated by an oxidized LDL-Tet-1-dependent epigenetic reprogramming of their gene expression within the HSC.[28]

These findings led us to hypothesize that hypercholesterolemia impairs collateral artery enlargement by a Tet1-dependent HSC-autonomous mechanism that increases the differentiation from HSCs into proinflammatory Ly6C^{hi} monocytes but restricts the conversion of Ly6C^{hi} monocytes into proangiogenic Ly6C^{low} monocytes in a murine model of limb ischemia.

METHODS

Mice. We purchased 8- to 12-week-old male C57BL/6J wild-type (WT), C57BL/6-Tg (UBC-GFP) 30scha/J (enhanced green fluorescent protein [EGFP]), and congenic CD45.1[+] (B6.SJL-Ptprca Pepcb/BoyJ) and ApoE^{−/−}

(B6.129P2-Apoe^{tm1Unc}/J) mice from Jackson Laboratories. Tet1$^{-/-}$ mice were generated by breeding Tet1 heterozygous mice. All mice were maintained in mouse barrier facilities. The care and use of the mice were in accordance with the National Institutes of Health guidelines, and the institutional animal care and use committee of the University of Massachusetts Medical School approved all mouse protocols. We induced hypercholesterolemia by feeding WT C57BL/6J mice a high cholesterol diet (HCD) for 2 months (D12108 C, containing 1.25% cholesterol; Research Diets). The cholesterol in normal mouse chow is 0.01% (ProLab RMH 3000 5P76; LabDiet). EGFP transgenic mice fed an HCD were used in HSC transplantation experiments to track the recruitment of intermediate or terminally differentiated daughter cells from donor HSCs in the ischemic limb of the recipient mice. Hindlimb ischemia was induced by femoral artery excision.

Identification, isolation, and transplantation of HSCs and monocytes. Mouse HSCs, defined as cKit$^+$sca-1$^+$CD90.1$^{-/low}$Lin$^-$ cells, were isolated from the bone marrow of tibias and femurs and maintained in minimum essential media, alpha modification (Sigma), containing 12.5% fetal calf serum (JRH Bioscience), 12.5% horse serum (Gibco BRL), and 1 nM dexamethasone. To expand cKit$^+$sca-1$^+$CD90.1$^{-/low}$Lin$^-$ cells, the media was supplemented with stem cell factor (10 ng/mL), thrombopoietin (10 ng/mL), FMS-like tyrosine kinase 3 (10 ng/mL), interleukin-3 (6 ng/mL), and interleukin-6 (10 ng/mL). Recipient mice were lethally irradiated in a cesium-137 irradiator, anesthetized, and transplanted with 3000 HSCs in 100 μL sterile phosphate-buffered saline via the retro-orbital plexus.[28] Limb ischemia was induced 2 months after HSC transplantation when hematopoiesis was fully reconstituted in the recipient mice.

Monocytes, defined as CD11b$^+$Ly6C^{hi} or CD11b$^+$Ly6C^{low} cells, were isolated from the bone marrow or peripheral blood. The transplantation model was used to determine the therapeutic potential of monocytes to increase collateral artery enlargement. The recipients were not irradiated. Monocytes were isolated and subsequently infused into the recipient's ischemic gastrocnemius and thigh muscles by intramuscular injection (5×10^5 in 100 μL sterile phosphate-buffered saline) 24 hours after the recipient mice underwent induction of limb ischemia. The source of antibodies is listed in Supplementary Table I.

Chromatin immunoprecipitation quantitative polymerase chain reaction. Chromatin immunoprecipitation (ChIP) was performed as follows: approximately 1×10^6 HSCs were incubated for 10 minutes at room temperature with 1% formaldehyde. After cross-linking, the reaction was quenched with 0.25 M glycine for 10 minutes at room temperature. Proteins were initially cross-linked to DNA, and nuclei were then pelleted and sonicated to 200-to 500-bp fragments (Bioruptor; Diagenode). The cross-linked DNA was immunoprecipitated with H3K4me3 antibody (Millipore) overnight at 4°C with rotation. DNA-antibody complexes were bound to ChIP beads, pulled down, washed, and eluted from beads. Following the reversal of cross-linkage, purified DNA was used for quantitative polymerase chain reaction (qPCR) using ChIP qPCR primers purchased from Integrated DNA Technologies. Immunoprecipitation efficiency was calculated by normalizing sample C_T (cycle threshold) values against control IgG values and calculating ratios of sample C_T values relative to input values.

DNA extraction, bisulfite conversion, and pyrosequencing. Genomic DNA was extracted from HSCs using standard phenol/chloroform extraction, followed by isopropanol precipitation and ethanol wash, and quantified using a NanoDrop spectrophotometer; 500 ng of DNA was used in the bisulfite conversion reactions where unmethylated cytosines were converted to uracil with the EZ DNA Methylation Gold kit (Zymo Research) according to the manufacturer's instructions. In brief, DNA was mixed with CT conversion reagents, and the conversion was run in a thermocycler (Biometra) at the recommended cycle conditions. Converted DNA was purified on a spin column and eluted into a total of 10 μL Buffer EB (Qiagen). PCR and pyrosequencing primer sets with one biotin-labeled primer were used to amplify the bisulfite-converted DNA. New primers for each gene were designed using PyroMark Assay Design software, version 2.0.1.15 (Qiagen). The size of the amplicons was approximately 100 to 200 bp.

PCRs were performed using a converted DNA by 2xHiFi Hotstart Uracil+Ready Mix RCR kit (Kapa Biosystems). In brief, 5 μL master mix, 5 pmol of each primer, 20 ng of genomic DNA, and ultrapure water to a final volume of 10 μL were mixed for each reaction and run at thermal cycling conditions: 95°C for 3 minutes and then 50 cycles: 20 seconds at 98°C, 15 seconds at the optimized primer-specific annealing temperature, 15 seconds at 72°C, and a final extension for 1 minute at 72°C. The amplified DNA was confirmed by electrophoresis in a 2% agarose gel. Next, 2 μL streptavidin beads (GE Healthcare), 40 μL PyroMark binding buffer, 10 μL PCR product, and 28 μL water were mixed and incubated for 10 minutes on a shaking table at 1300 rpm. Using the Biotage Q96 Vacuum Workstation, amplicons were separated, denatured, washed, and added to 25 μL annealing buffer containing 0.33 μM of pyrosequencing primer. Primer annealing was performed by incubating the samples at 80°C for 2 minutes and allowed to cool to room temperature before pyrosequencing. PyroGold reagents were used for the pyrosequencing reaction, and the signal was analyzed using the PSQ-96MA system (Biotage). Target CGs
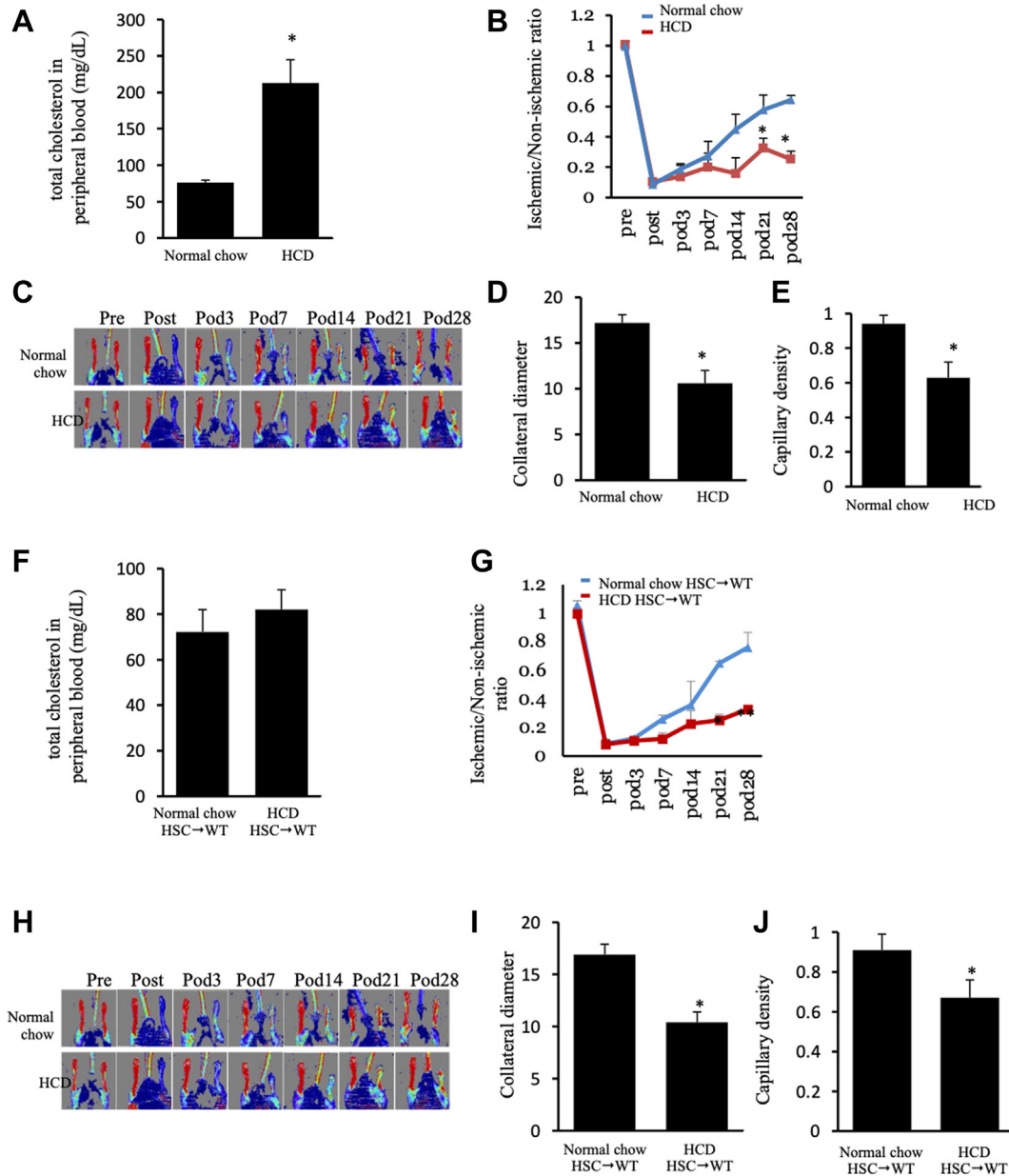
Fig 1. Blood flow recovery and postischemic neovascularization are impaired in high cholesterol diet (HCD)-induced hypercholesterolemic mice and wild-type (WT) recipients transplanted with hematopoietic stem cells (HSCs) from hypercholesterolemic mice. **A,** Cholesterol level in peripheral blood of recipient mice. **B,** Blood flow recovery in recipient mice after induction of hindlimb ischemia. **C,** Representative images of laser Doppler perfusion imaging (LDPI). **D,** Collateral artery diameter in ischemic muscles of recipient mice 28 days after induction of hindlimb ischemia. **E,** Capillary density in ischemic muscles of recipient mice 28 days after induction of hindlimb ischemia. **F,** Cholesterol levels in peripheral blood of HCD mice. **G,** Blood flow recovery in WT recipient mice after induction of hindlimb ischemia. **H,** Representative images of LDPI. **I,** Collateral artery diameter in ischemic muscles of WT recipient mice 28 days after induction of hindlimb ischemia. **J,** Capillary density in ischemic muscles of WT recipient mice 28 days after induction of hindlimb ischemia. (**A-G**, n = 11; **H-J**, n = 10; **A, D-F, I, J,** unpaired *t*-test; **B, G,** one-way analysis of variance; *$P < .05$ vs normal chow mice. *$P < .05$ vs WT recipient mice transplanted with HSCs from standard chow mice.) *POD,* Postoperative day.

were evaluated by instrument software (PSQ-96MA, version 2.1; Biotage) which converts the programs to numerical values for peak heights and calculates the percentage of methylation at each base as a Cycles Threshold ratio.

Statistical analysis. Statistical analyses were performed with GraphPad Prism software. Statistical significance was evaluated using one- or two-way analysis of variance or an unpaired *t*-test. Significance was set at $P < .05$. All experiments for which the results are non-normally
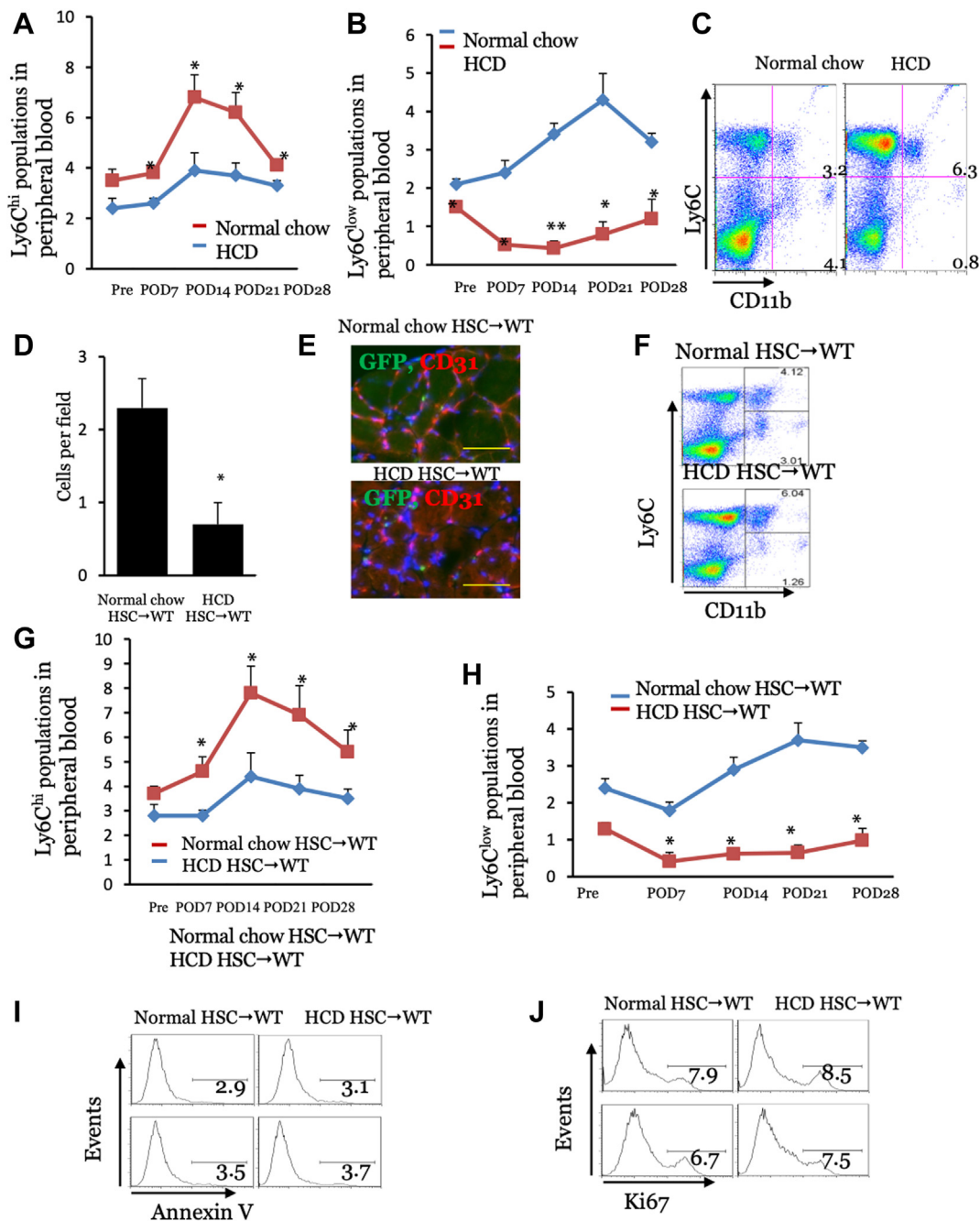
Fig 2. Effect of hypercholesterolemia hematopoietic stem cell (HSC) differentiation toward monocyte subsets is recapitulated in wild-type (WT) mice reconstituted with HSCs from hypercholesterolemic mice. **A,** Dynamic frequency of Ly6C^{hi} monocytes in peripheral blood after induction of hindlimb ischemia. **B,** Dynamic frequency of Ly6C^{low} monocytes in peripheral blood after induction of hindlimb ischemia. **C,** Representative fluorescence-activated cell sorting (FACS) analysis of monocytes in peripheral blood on day 28 after induction of hindlimb ischemia. **D,** Number of green fluorescent protein-positive (*GFP+*) HSC-derived endothelial cells in ischemic tissues. **E,** Representative images of the GFP+ HSC-derived endothelial cells incorporated into the vasculature of ischemic tissues (scale bar, 100 μm). **F,** Representative FACS plots of monocytes in peripheral blood on day 28 after induction of hindlimb ischemia. **G,** Dynamic frequency of Ly6C^{hi} monocytes in peripheral blood after induction of hindlimb ischemia. **H,** Dynamic frequency of Ly6C^{low} monocytes in peripheral blood after induction of hindlimb ischemia. **I,** Apoptotic population in Ly6C^{hi} and Ly6C^{low} monocyte subsets. **J,** Proliferative population in Ly6C^{hi} and Ly6C^{low} monocyte subsets. (**A-G,** n = 11; **H-J,** n = 10; **D, I, J,** unpaired *t*-test; **C, F, G, I,** one-way analysis of variance; *$P < .05$ vs normal chow mice; *$P < .05$ vs WT recipient mice transplanted with HSCs from standard chow mice.) *POD,* Postoperative day.

distributed (eg, percent change) were analyzed using appropriate nonparametric tests, including the Wilcoxon signed rank test and Mann-Whitney *U* test for multiple comparisons.

RESULTS

To establish a direct cause-and-effect relationship between hypercholesterolemia and impaired collateral artery enlargement, we generated a hypercholesterolemic mouse model by feeding WT C57BL/6J mice an HCD. Their cholesterol level reached 213 ± 32 mg/dL in the peripheral blood (Fig 1, *A*). The cholesterol level in the standard chow group was 76 ± 5 mg/dL. At 28 days after the induction of hindlimb ischemia, blood flow recovery was 2.6-fold lower in the HCD mice than in the standard chow mice (Fig 1, *B and C*). In concordance with this blood flow deficit, the collateral artery diameters and capillary density in the ischemic muscle of HCD mice were also significantly less than those in standard chow mice (Fig 1, *D and E*). Interestingly, in the peripheral circulation of standard chow mice, the frequency of Ly6C^{hi} monocytes was increased after induction of hindlimb ischemia and remained elevated at 28 days (Fig 2, *A and C*). In the HCD mice, the frequency of Ly6C^{hi} monocytes was substantially higher than that in standard chow mice at all time points (Fig 2, *A and C*). In the peripheral circulation of standard chow mice, the Ly6C^{low} monocytes doubled in number after the induction of limb ischemia and remained elevated to day 28 (Fig 2, *B and C*). In contrast, in the HCD mice, the frequency of Ly6C^{low} monocytes decreased after the induction of limb ischemia and remained at a significantly lower level throughout postischemic neovascularization (Fig 2, *B and C*), showing that hypercholesterolemia increases the population of Ly6C^{hi} monocytes but decreases the population of proangiogenic Ly6C^{low} monocytes.

To test the possibility that hypercholesterolemia impairs collateral artery enlargement by an HSC-autonomous mechanism, HSCs were isolated from EGFP CD45.2^{+} mice (C57BL/6-Tg(CAG-EGFP)131Osb.LeySopJ), which were fed an HCD and transplanted into lethally irradiated standard chow CD45.1^{+} recipients. The total serum cholesterol levels in the peripheral blood were similar in the standard chow recipient mice transplanted with HSCs from either standard chow or HCD mice (Fig 1, *F*). However, the lethally irradiated standard chow recipient mice reconstituted with HSCs from HCD mice displayed a reduction in blood flow recovery nearly identical to that in HCD mice despite the absence of hypercholesterolemia (Fig 1, *G and H*). Similarly, the mean collateral diameter in the thigh muscles and the mean capillary density in the ischemic muscle of these WT chimeric mice were also significantly reduced (Fig 1, *I and J*) despite the absence of hypercholesterolemia. Together, these results show that the deleterious effects of hypercholesterolemia on collateral artery enlargement and capillary density are due to an HSC-autonomous mechanism.

Based on these results, we hypothesized that hypercholesterolemia increases the differentiation of HSCs toward Ly6C^{hi} monocytes and restricts the conversion of Ly6C^{hi} monocytes toward Ly6C^{low} monocytes by an HSC-autonomous mechanism. To test this hypothesis, we isolated HSCs from EGFP mice in which hypercholesterolemia was induced with an HCD. We transplanted these HSCs into lethally irradiated WT recipient mice fed a standard chow diet. Monocytes induce arteriogenesis by secretion of cytokines, chemokines, and metalloproteases and transdifferentiation into vascular cells.[29] In these WT recipient mice, the incorporation of donor HSC-derived cells into the vasculature of the ischemic muscle was substantially less than that observed in WT mice reconstituted with HSCs from WT mice (Fig 2, *D and E*). Flow cytometry analysis showed a dynamic change in the frequency of Ly6C^{hi} and Ly6C^{low} monocytes in the peripheral circulation after the induction of hindlimb ischemia (Fig 2, *F*). In the lethally irradiated WT recipient mice reconstituted with HSCs isolated from mice fed standard chow, the frequency of Ly6C^{hi} monocytes increased immediately after the induction of limb ischemia, peaked about 14 days later, and then gradually decreased to basal levels. In contrast, Ly6C^{low} monocytes gradually increased and peaked 21 days after the induction of hindlimb ischemia (Fig 2, *G and H*). This pattern of changes in the Ly6C^{hi}/Ly6C^{low} frequency mirrored that of the nontransplanted hypercholesterolemic mice (Fig 2, *A and B*). In the WT recipient mice reconstituted with HSCs from HCD mice, the frequency of Ly6C^{hi} monocytes increased abruptly after the induction of hindlimb ischemia, and this frequency was sustained at significantly greater levels than that in the recipient standard chow mice reconstituted with HSCs from standard chow EGFP mice (Fig 2, *G and H*). Moreover, in mice transplanted with HSCs from mice consuming a HCD, the frequency of Ly6C^{low} monocytes decreased after the induction of hindlimb ischemia and remained significantly lower throughout the postischemic neovascularization process (Fig 2, *G and H*). These changes in the dynamic response in Ly6C^{hi} and Ly6C^{low} monocyte subpopulations were not due to variations in the induction of apoptosis or their proliferation rates (Fig 2, *I and J*). These results indicate that hypercholesterolemia induces an HSC-autonomous mechanism that increases HSC differentiation toward Ly6C^{hi} monocytes and restricts the conversion of Ly6C^{hi} monocytes into Ly6C^{low} monocytes during collateral artery enlargement.

To determine the proangiogenic function of the different monocyte subsets, we isolated Ly6C^{low} and Ly6C^{hi} monocytes from peripheral blood and bone marrow. We measured their proangiogenic functions both in vitro and in vivo. In vitro differentiation assays
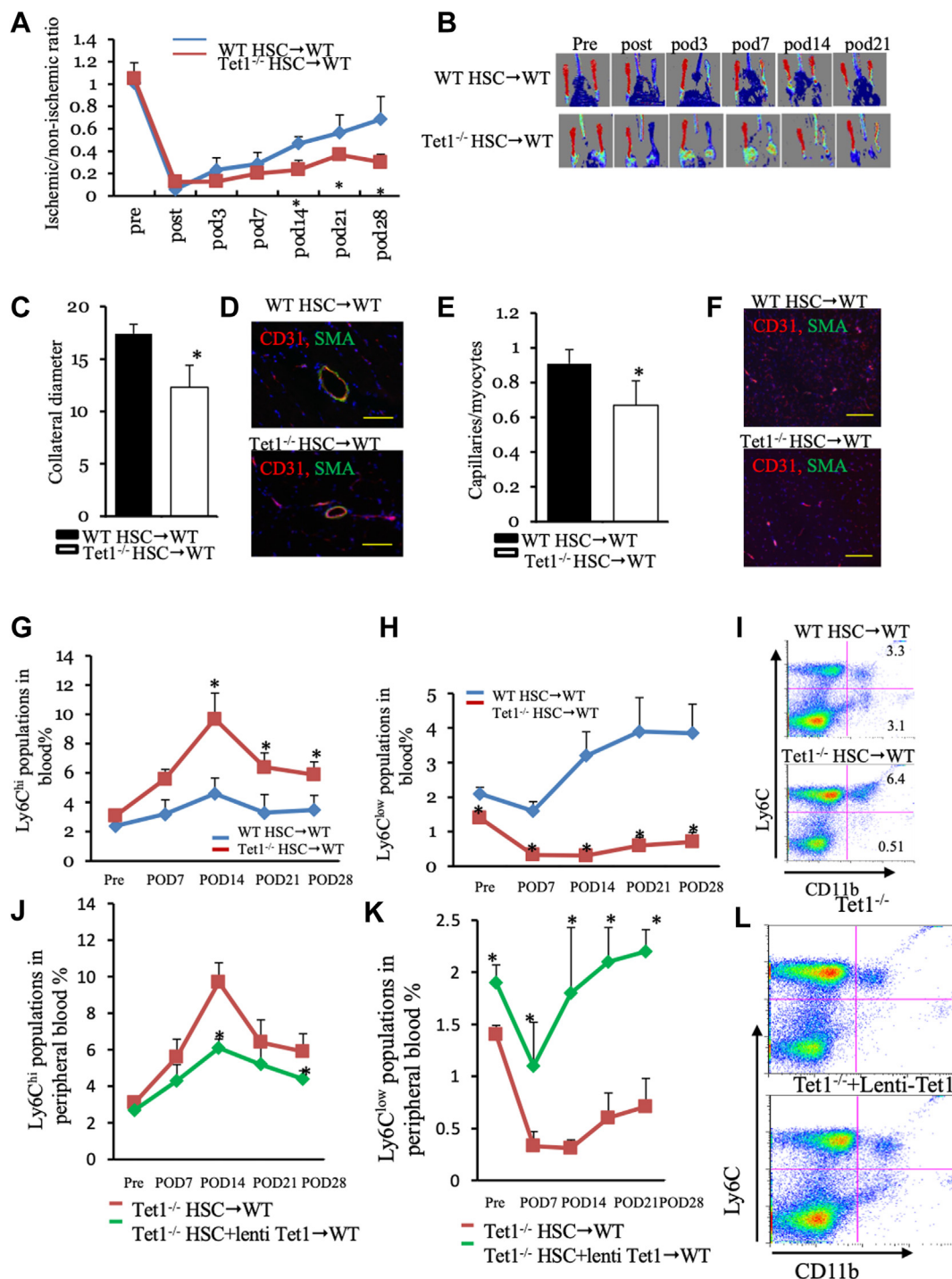
Fig 3. Ten-eleven translocation 1 (Tet1) deficiency in hematopoietic stem cells (HSCs) impairs postischemic neovascularization and HSC differentiation toward Ly6C^{low} monocytes. **A,** Blood flow recovery of recipient mice after induction of hindlimb ischemia. **B,** Representative images of laser Doppler perfusion imaging (LDPI). **C,** Collateral artery diameter in ischemic muscles of recipient mice 28 days after induction of hindlimb ischemia. **D,** Representative images of collateral artery. **E,** Capillary density in ischemic muscles of recipient mice 28 days after induction of hindlimb ischemia. **F,** Representative images of capillaries. **G,** Dynamic frequency of Ly6C^{hi} monocytes in peripheral blood after induction of hindlimb ischemia. **H,** Dynamic frequency of Ly6C^{low} monocytes in peripheral blood after induction of hindlimb ischemia. **I,** Representative fluorescence-activated cell sorting (FACS) plots of monocytes in peripheral blood on day 28 after induction of hindlimb ischemia. **J,** Dynamic frequency of Ly6C^{hi} monocytes in peripheral blood after induction of hindlimb ischemia. **K,** Dynamic frequency of Ly6C^{low} monocytes in peripheral blood after induction of hindlimb ischemia. **L,** Representative FACS plots of monocytes in peripheral blood on day 28 after induction of hindlimb ischemia. (**A-L,** n = 10; **C,F,** unpaired *t-* test; **A,G,H,J,K,** analysis of variance; *$P < .05$ vs WT recipient mice transplanted with HSCs from WT mice; *$P < .05$ vs WT recipient mice transplanted with Tet1$^{-/-}$ HSCs.) *pod,* Postoperative day; *SMA,* smooth muscle actin.

showed that the Ly6C^{low} monocytes isolated from peripheral blood had the greatest potential to differentiate into CD144$^+$ endothelial cells (Supplementary Fig 1, *A*) and smooth muscle cells (Supplementary Fig 1, *B*) and to incorporate in vitro into tubules formed by endothelial cells (Supplementary Fig 1, *C and D*). Interestingly, Ly6C^{hi} monocytes isolated from bone marrow showed a higher differentiation potential than did Ly6C^{hi} monocytes from the peripheral circulation and Ly6C^{low} monocytes from the bone marrow, suggesting that the function of the monocyte subsets is context specific (Supplementary Fig 1). To test their proangiogenic potential in vivo, in separate experiments, we infused the two monocyte subsets into standard chow mice 24 hours after induction of hindlimb ischemia. The recipient mice infused with either Ly6C^{low} monocytes from peripheral blood or Ly6C^{hi} monocytes from the bone marrow showed greater blood flow recovery, collateral diameters, and capillary density. In contrast, the recipient mice infused with either peripheral blood Ly6C^{hi} monocytes or bone marrow Ly6C^{low} monocytes did not show any improvement in these variables beyond the control values (Supplementary Fig 2). These results suggest that Ly6C^{low} monocytes in the peripheral blood function as the major cellular component that induces collateral artery enlargement during postischemic neovascularization.

Although Tet enzymes are involved in various physiological and pathological processes, it is unknown whether they regulate collateral artery enlargement. Our previous study showed that hypercholesterolemia induced an oxidant stress-dependent reduction of the expression of Tet1 in HSCs from hypercholesterolemic ApoE$^{-/-}$ mice that reduced the frequency of NKT and $\gamma\delta$ T cells, which, in turn, impaired cancer immunosurveillance and increased the number and pathological severity of colorectal tumors.[28] In agreement with these findings, hypercholesterolemia induced by an HCD also reduced the expression of Tet1 in HSCs (Supplementary Fig 3). Our findings show that the effects of hypercholesterolemia on collateral artery enlargement are mediated by an HSC-autonomous mechanism. Therefore, we hypothesized that hypercholesterolemia induces a Tet1-dependent epigenetic reprogramming of monocyte gene expression within the HSCs, reducing their differentiation toward proangiogenic Ly6C^{low} monocytes and impairing collateral artery enlargement. To test this hypothesis, HSCs were isolated from Tet1$^{-/-}$ CD45.2$^+$ mice and transplanted into lethally irradiated standard chow CD45.1$^+$ mice. These chimeric mice showed a significant impairment in blood flow recovery after induction of hindlimb ischemia, like that observed in non-transplanted HCD mice (Fig 3, *A and B*). In WT CD45.1$^+$ recipient mice reconstituted with HSCs isolated from Tet1$^{-/-}$ CD45.2$^+$ mice, both the collateral artery diameter (Fig 3, *C and D*) and the capillary density were significantly lower than in those reconstituted

with WT HSCs (Fig 3, *E* and *F*). In standard chow CD45.1$^+$ mice reconstituted with Tet1$^{-/-}$ HSCs, the frequency of Ly6C^{hi} monocytes abruptly increased after the induction of hindlimb ischemia. It remained higher, nearly identical to that in hypercholesterolemic mice (Fig 3, *G-I*). In contrast, in mice transplanted with Tet1$^{-/-}$ HSCs, the frequency of Ly6C^{low} monocytes decreased after the induction of hindlimb ischemia and remained at a significantly lower level throughout postischemic neovascularization, again very similar to that of the HCD mice (Fig 3, *H and I*). Next, we overexpressed the catalytic domain of Tet1 in Tet1$^{-/-}$ HSCs. Based on our previous observation that overexpression of Tet1 in HSCs impairs their bone marrow engraftment, these HSCs that overexpress Tet1 were transplanted together with standard chow CD45.1$^+$ HSCs at a ratio of 1:1 to restore their capacity to engraft into the bone marrow.[28] In the recipient WT mice reconstituted with HSCs in which Tet1 expression was restored by lentiviral-mediated transduction, the frequency of Ly6C^{hi} monocytes was lower than in those transplanted with Tet1$^{-/-}$ HSCs throughout the period of blood flow recovery (Fig 3, *J*). At the same time, the frequency of Ly6C^{low} monocytes was significantly higher after the induction of hindlimb ischemia in the standard chow mice in which Tet1 expression was restored than in the standard chow mice transplanted with Tet1$^{-/-}$ HSCs (Fig 3, *K and L*). These results indicate, to the best of our knowledge, for the first time, that Tet1 regulates the differentiation of HSCs toward Ly6C^{hi} and Ly6C^{low} monocytes. Hypercholesterolemia downregulates Tet1 in HSCs, subsequently increasing their differentiation toward proinflammatory Ly6C^{hi} monocytes and restricting their conversion into proangiogenic Ly6C^{low} monocytes, substantially impairing collateral artery enlargement.

To determine the molecular mechanism by which hypercholesterolemia-induced downregulation of Tet1 impairs their differentiation toward Ly6C^{low} monocytes, we measured the monocyte "fingerprint genes" described in a previous study[30] and the critical regulatory genes in the differentiation process from HSCs toward monocytes (Supplementary Table II; Fig 4). We isolated monocytes and HSCs from lethally irradiated WT mice transplanted with WT or Tet1$^{-/-}$ HSCs. The expression of c-Jun in Ly6C^{low} monocytes from mice transplanted with Tet1$^{-/-}$ HSCs was threefold greater than that in WT mice reconstituted with WT HSCs (Fig 4, *A*). In contrast, the expression of p65, STAT4, VDR, MCP1, PDGFβ, bFGF, IRF1, IRF8, KLF2, SDF1, and GATA6 was significantly lower than that in the Ly6C^{low} monocytes from mice transplanted with WT HSCs (Fig 4, *B*). Consistent with our hypothesis, the expression of these genes displayed a nearly identical expression profile in the HSCs isolated from mice reconstituted with Tet1$^{-/-}$ HSCs (Fig 4, *C and D*), indicating that the expression of
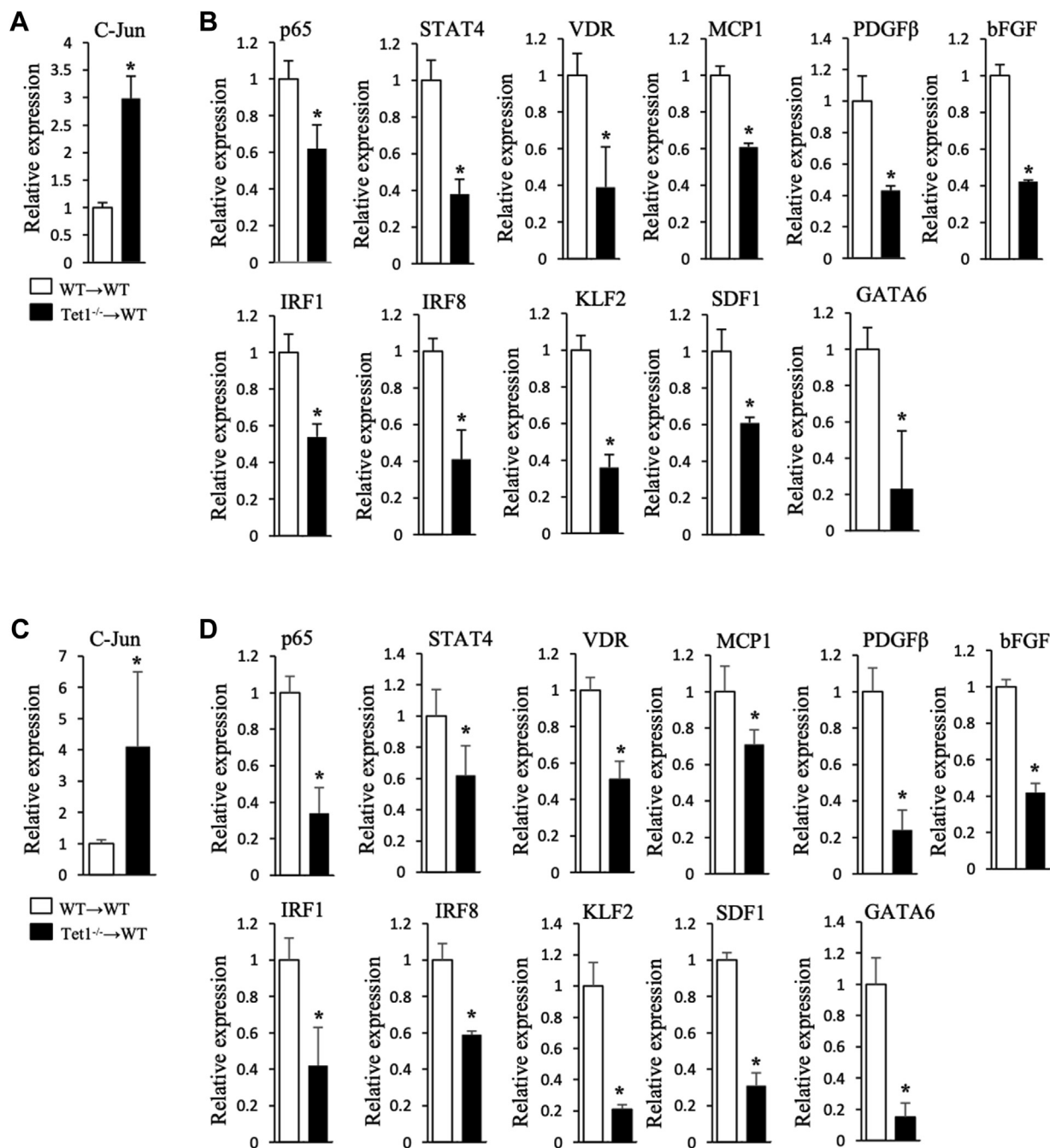
Fig 4. The genes related to monocyte differentiation show differential expression in Ly6C^low monocytes derived from ten-eleven translocation 1 (Tet1)^−/− hematopoietic stem cells (HSCs) and in Tet1^−/− HSCs. **A,** Upregulated genes in Ly6C^low monocytes. **B,** Downregulated genes in Ly6C^low monocytes. **C,** Upregulated genes in HSCs. **D,** Downregulated genes in HSCs. (n = 6; Wilcoxon signed rank test and Mann-Whitney U test for multiple comparisons; *$P < .05$ vs Ly6C^low monocytes derived from wild-type [WT] HSCs.)

these genes is first epigenetically reprogrammed in HSCs and then carried down through differentiation into terminally differentiated monocytes.

Because Tet-dependent DNA demethylation typically increases the transcription of target genes, we next sought to characterize the changes in DNA methylation at the regulatory regions of the genes whose expression was changed in the Ly6C^low monocytes derived from Tet1^−/− HSCs. Multiple hypermethylated CpG islands were found in the regulatory regions of IRF1, PDGFβ, MCP1, p65, STAT4, IRF8, and VDR in Ly6C^low monocytes (Fig 5, A). Because Ly6C^low monocytes were also reduced in the WT recipient mice reconstituted with Tet1^−/− HSCs, we further tested the possibility that these repressive
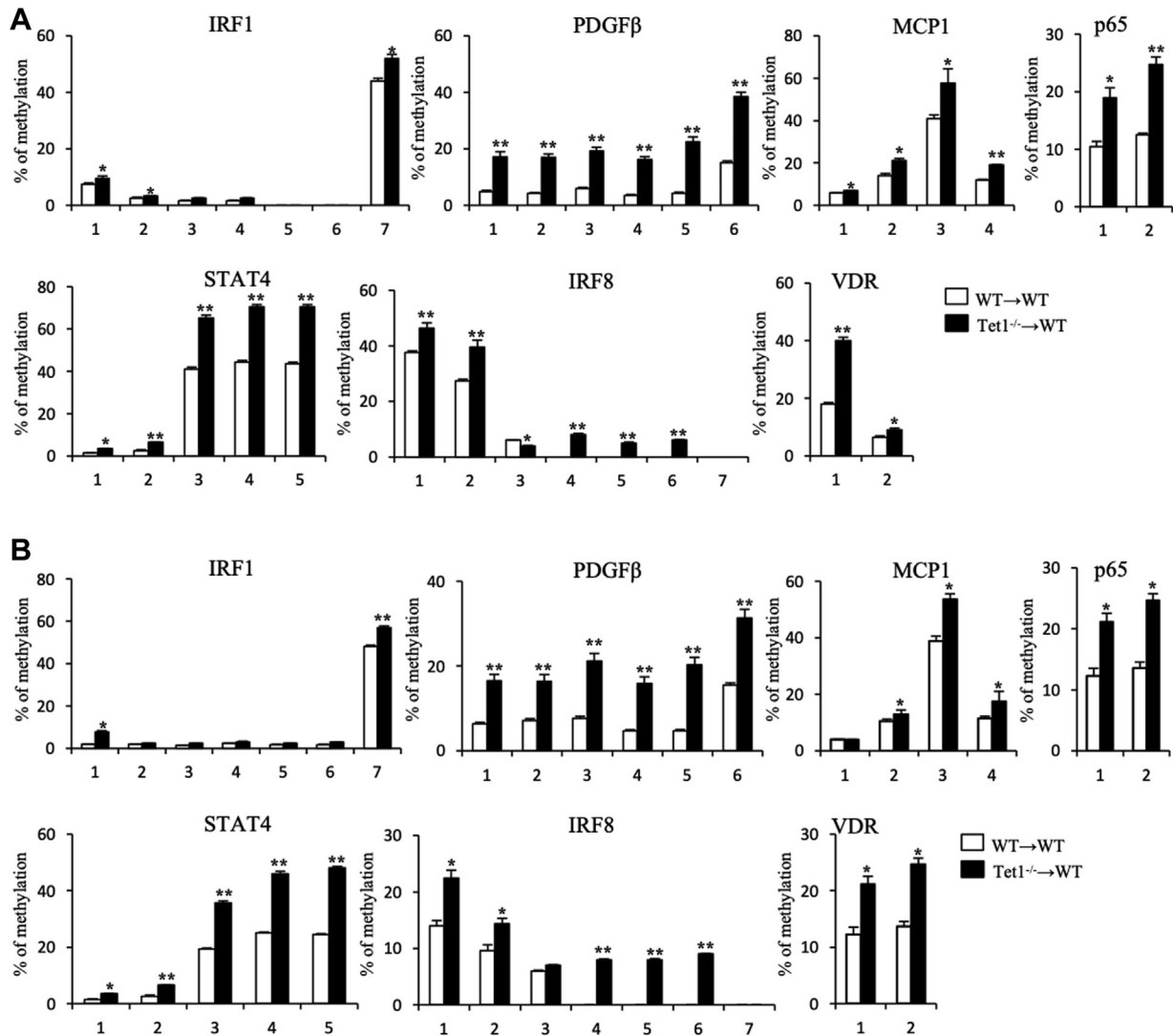
Fig 5. Ten-eleven translocation 1 (Tet1) deficiency increases the DNA methylation status of the genes critical in the differentiation of Ly6C^{low} monocytes. **A,** DNA methylation status of the genes in Ly6C^{low} monocytes derived from wild-type (WT) and Tet1$^{-/-}$ hematopoietic stem cells (HSCs; n = 6; *$P < .05$ vs Ly6C^{low} monocytes derived from WT mice). **B,** DNA methylation status of the genes in WT and Tet1$^{-/-}$ HSCs (n = 6; Wilcoxon signed rank test and Mann-Whitney U test for multiple comparisons. *$P < .05$ vs WT HSCs).

DNA methylation marks were first reprogrammed in HSCs and then carried down through differentiation to terminally differentiated monocytes. In fact, the hyper-methylation status of these genes was nearly identical in HSCs isolated from mice transplanted with Tet1$^{-/-}$ HSCs (Fig 5, *B*). This finding shows that the effect of hy-percholesterolemia on the gene expression and methyl-ation pattern of terminally differentiated monocytes is not due to the direct effect of hypercholesterolemia on these terminally differentiated immune cells. Rather, it is due to hypercholesterolemia-induced epigenetic reprogramming of their gene expression within HSCs.

Tet proteins also participate in the regulation of histone modifications via distinct pathways.[28,29,31] Therefore, we determined the effect of Tet1 on histone modification of the described genes. H3K4me3 is a histone modifica-tion that increases the expression of genes, and we, and others, have shown that Tet1 facilitates the methyl-ation of H3K4me3.[28,32] In Ly6C^{low} monocytes derived from Tet1$^{-/-}$ HSCs, ChIP-PCR analysis showed that the H3K4me3 modification was significantly decreased in KLF2, bFGF, PDGFβ, SDF1, GATA6, and STAT4 (Fig 6, *A*). Similarly, in Tet1$^{-/-}$ HSCs, KLF2, bFGF, PDGFβ, SDF1, GATA6, and STAT4 also showed significant decreases in the Tet-induced H3K4me3 modification (Fig 6, *B*). In contrast, c-Jun showed a significant decrease in H3K27me3, a repressive histone modification (Fig 6, *C* and *D*), supporting the increased expression of c-Jun in both Ly6C^{low} monocytes and HSCs. Thus, Tet1 induces a bivalent regulation of gene expression and chromatin
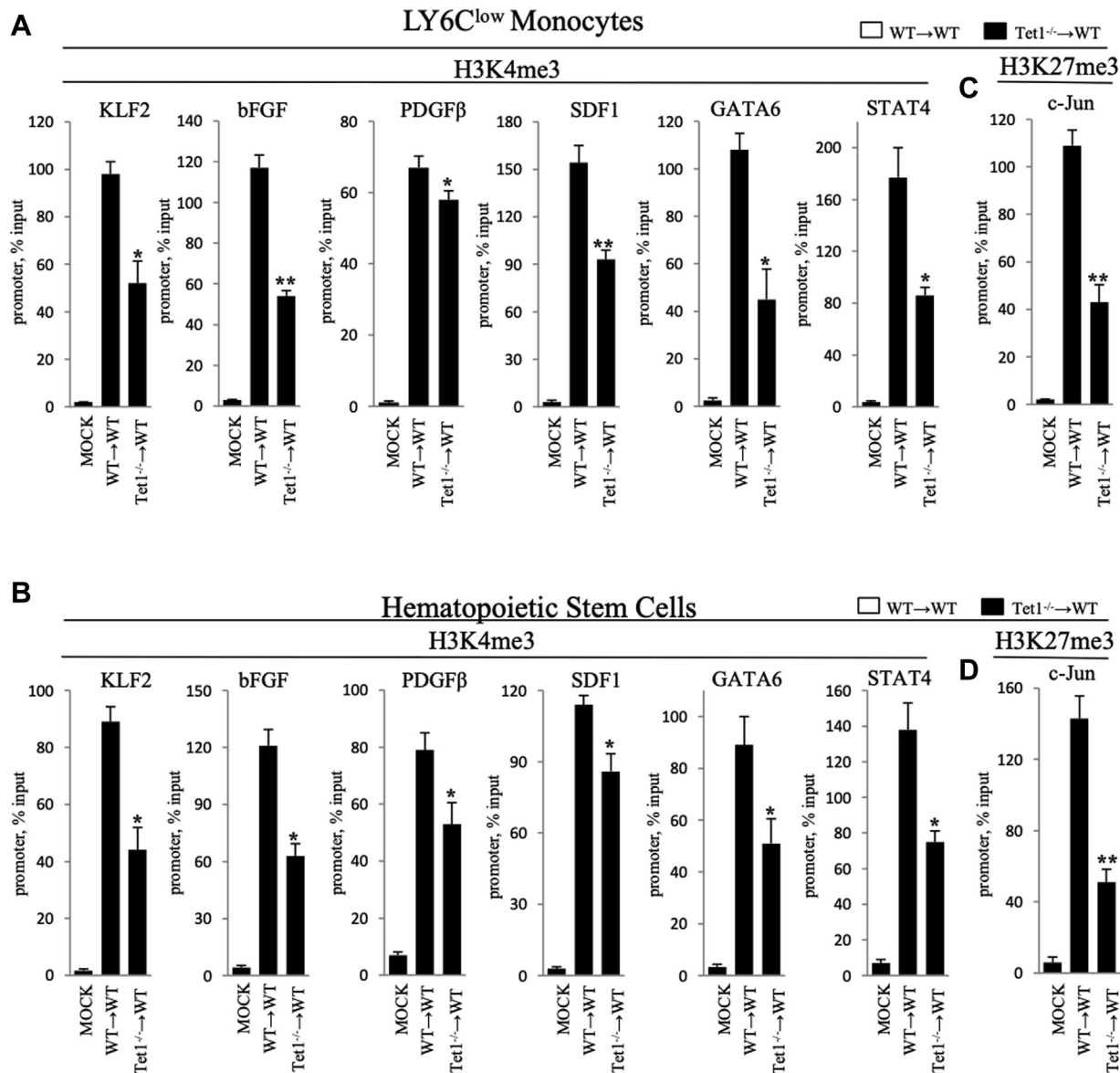
Fig 6. Ten-eleven translocation 1 (Tet1) deficiency decreases the H3K4me3 or H3K27me3 modifications of the genes critical in the differentiation of Ly6C^low monocytes. **A,** H3K4me3 modification of downregulated genes in Ly6C^low monocytes derived from wild-type (WT) and Tet1^−/− hematopoietic stem cells (HSCs; n = 6; *P < .05, vs Ly6C^low monocytes derived from WT HSCs [WT→WT]). **B,** H3K4me3 modification of downregulated genes in HSCs of WT and Tet1^−/− mice (n = 6; *P < .05 vs HSCs of WT mice). **C,** H3K27me3 modification of c-Jun in Ly6C^low monocytes derived from WT and Tet1^−/− HSCs (n = 6; *P < .05 vs Ly6C^low monocytes derived from WT HSCs [WT→WT]). **D,** H3K4me3 modification of c-Jun in WT and Tet1^−/− HSCs (n = 6; Wilcoxon signed rank test and Mann-Whitney *U* test for multiple comparisons; *P < .05 vs WT HSCs).

remodeling of these genes, which occur first in the HSCs and are then carried down through differentiation into terminally differentiated cells.

To determine whether the genes responsible for monocyte differentiation have a similar pattern of expression and methylation status in HSCs and Ly6C^low monocytes from HCD mice to that of Tet1^−/− mice, HSCs and Ly6C^low monocytes were isolated from WT and HCD mice. Gene expression and DNA methylation status were measured.

We found that the genes responsible for monocyte differentiation have a similar pattern of expression and methylation status in HSCs and Ly6C^low monocytes from HCD mice to that of Tet1^−/− mice (Supplementary Figs 4 and 5).

To determine in vivo whether restoration of Tet1 expression in HCD HSCs can restore blood flow recovery in hypercholesterolemic mice in response to hindlimb ischemia, we transplanted HCD HSCs that overexpressed
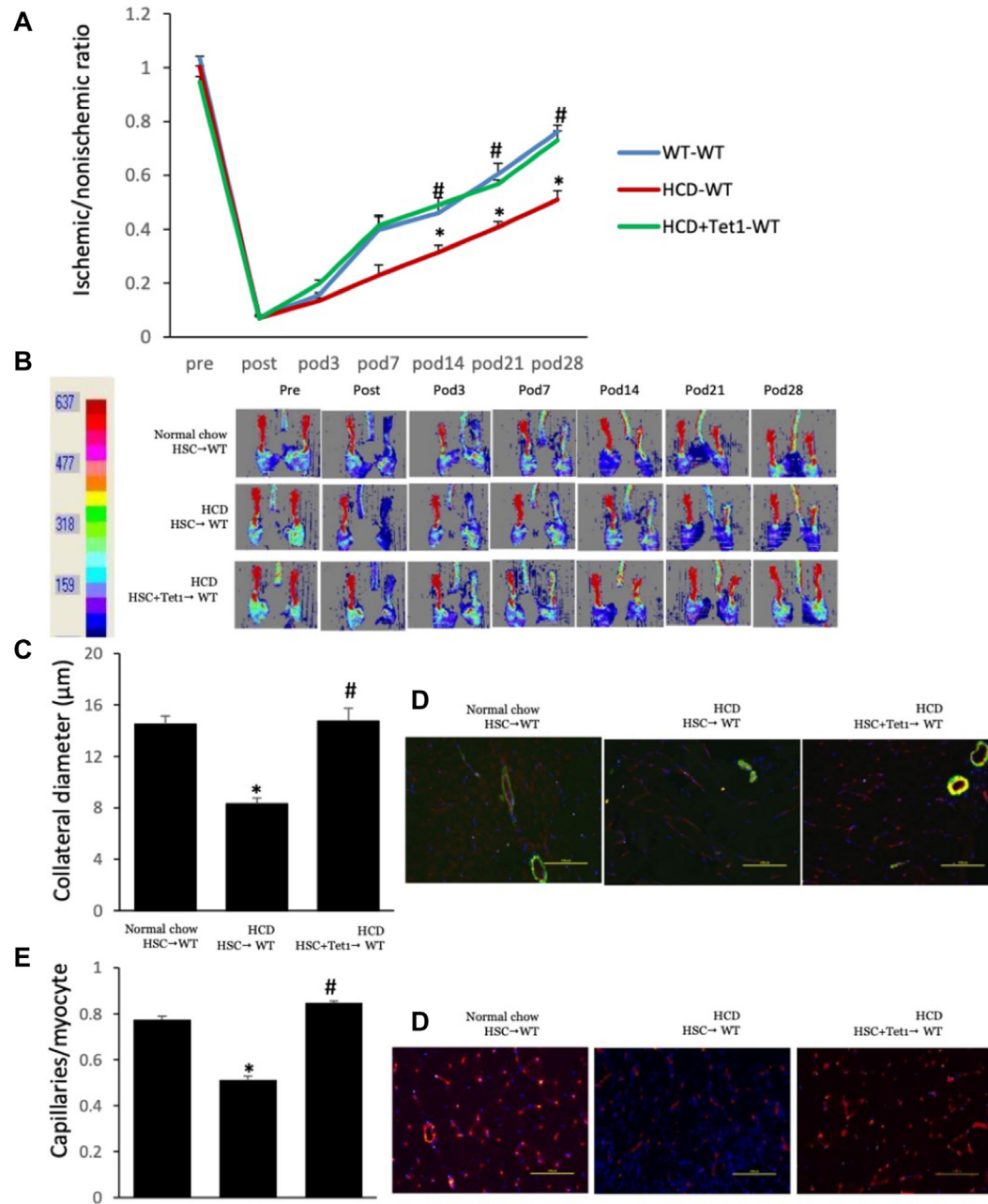
Fig 7. Overexpression of ten-eleven translocation 1 (Tet1) in high cholesterol diet (HCD) hematopoietic stem cells (HSCs) restores collateral artery enlargement in response to hindlimb ischemia in hypercholesterolemic mice. **A,** Blood flow recovery in recipient mice after induction of hindlimb ischemia. **B,** Representative images of laser Doppler perfusion imaging (LDPI). **C,** Collateral artery diameter in ischemic muscles of recipient mice 28 days after induction of hindlimb ischemia. **D,** Capillary density in ischemic muscles of recipient mice 28 days after induction of hindlimb ischemia (n = 4; *$P <$ .05 vs WT recipient mice transplanted with HSCs from normal chow mice; Wilcoxon signed rank test and Mann-Whitney *U* test for multiple comparisons; #$P <$ .05 vs WT recipient mice transplanted with HSCs from HCD mice). *Pod,* Postoperative day.

Tet1 into lethally irradiated WT recipients and then induced hindlimb ischemia 2 months after HSC transplantation and reconstitution of hematopoiesis. We found that blood flow recovery was significantly increased in WT recipients transplanted with either WT HSCs or Tet1 overexpression HCD HSCs (Fig 7, *A* and *B*).

In fact, similar to the results of gene expression and epigenetic marks, the blood flow recovery was identical to that of WT mice. The collateral artery diameters and capillary density of WT recipients transplanted with HSCs from HCD mice that overexpressed Tet1 were also significantly increased and were even higher than those
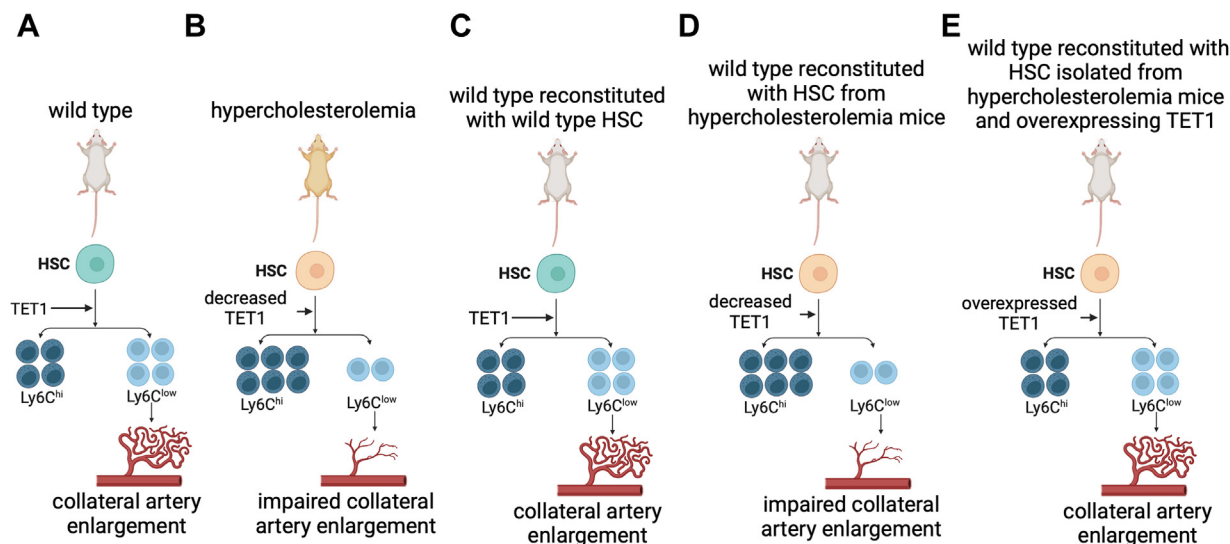
Fig 8. Hypercholesterolemia impairs collateral artery enlargement by a ten-eleven translocation 1 (Tet1)-dependent hematopoietic stem cell (HSC)-autonomous mechanism. **A,** Collateral artery enlargement is regulated by the ratio of inflammatory (Ly6C^{hi}) and angiogenic (Ly6C^{low}) monocyte subsets. **B,** Hypercholesterolemia impairs collateral artery enlargement by downregulating Tet1, which increases the Ly6C^{hi} monocyte subset and reduces the Ly6C^{low} subset. **C,** When lethally irradiated wild-type (WT) mice are reconstituted with WT HSCs, the monocyte subsets are unchanged, and collateral artery enlargement proceeds normally. **D,** When lethally irradiated WT mice are reconstituted with HSCs from hypercholesterolemic mice, collateral artery enlargement proceeds as it does in hypercholesterolemic mice, consistent with an HSC-autonomous mechanism. **E,** When lethally irradiated WT mice are reconstituted with HSCs from hypercholesterolemic mice with restored Tet1 expression, collateral artery enlargement proceeds as it does in WT mice, confirming the Tet1-dependent HSC-autonomous mechanism.

of WT mice reconstituted with WT HSCs (Fig 7, C-F). These findings indicate that the effects of hypercholesterolemia on postischemic neovascularization are due to a Tet1-dependent HSC-autonomous mechanism in which the number and gene expression of monocytes are epigenetically reprogrammed within the HSCs.

DISCUSSION

These results indicate that after the induction of hindlimb ischemia, collateral artery enlargement and capillary density are regulated by an HSC-autonomous mechanism whereby Tet1 is a master regulator in the fate decision of HSC differentiation toward Ly6C^{hi} and Ly6C^{low} monocytes. Hypercholesterolemia alters these cell fate decisions by downregulating Tet1 in HSCs, which increases their lineage priming toward proinflammatory Ly6C^{hi} monocytes and reduces their conversion into proangiogenic Ly6C^{low} monocytes (Fig 8). This disrupts the dynamic frequency of these monocyte subsets during postischemic neovascularization (Fig 2, A and B). These deleterious effects of Tet1$^{-/-}$ on the critical regulatory genes in the differentiation process of HSCs toward monocytes and their angiogenic function are epigenetically reprogrammed in HSCs and then carried down through differentiation into terminally differentiated monocytes. Consistent with this conclusion, these genes displayed an identical expression profile and epigenetic

marks in the HSCs and monocytes isolated from WT mice reconstituted with either WT or Tet1$^{-/-}$ HSCs, indicating an HSC-autonomous mechanism (Figs 4 and 5).

Our finding that collateral artery enlargement is regulated by an oxidant stress-dependent HSC-autonomous mechanism differs fundamentally from the current paradigm centered exclusively on flow-mediated endothelial cell activation and nitric oxide-mediated collateral artery remodeling.[33,34] In this traditional paradigm, activated endothelial cells release chemoattractants that mobilize monocytes from the bone marrow and promote their entry into the perivascular space, where they release growth factors and cytokines that drive collateral artery remodeling. These monocytes also transdifferentiate into endothelial and smooth muscle cells (Supplementary Fig 1). Under pathological conditions, hypercholesterolemia causes an oxidized LDL-dependent increase in endothelial cell oxidant stress that initiates endothelial dysfunction. In parallel, we have shown that hypercholesterolemia also induces an oxidized LDL increase in HSC-oxidant stress that initiates the pathological signaling pathway, culminating in the downregulation of Tet1.[35] The similarities of these pathological responses should not be unexpected. Endothelial cells and HSCs are derived from the aorta-gonadal mesonephros, which first differentiates into endothelial cells, and then, after developing in the circulation, the

endothelial cells differentiate into HSCs.[36] Both are relatively resistant to hypoxia and exquisitely sensitive to oxidant stress. Finally, both use adenosine triphosphate anaerobically via glycolysis but switch to oxidative phosphorylation for rapid cell proliferation.

The Tet family of methylcytosine dioxygenases catalyzes the hydroxylation of 5- methylcytosine and transforms it into 5-hydroxymethylcytosine (5hmC); 5hmC is associated with transcriptionally activated and transcriptionally repressed gene subsets and is a critical epigenetic code in diverse physiological and pathological processes. It has been reported that Tet1 and Tet2 mRNA expression levels were substantially downregulated in ischemia—reperfusion-afflicted kidneys.[37] Additionally, ischemia—reperfusion injury decreased the 5hmC enrichment of *Cxcl10* and *Ifngr2* genes, but the transcription of these two genes increased. *Cxcl10* is expressed by endothelial cells in response to inflammatory stimuli and is believed to mediate leukocyte recruitment during inflammation.[37] These previous findings suggest that the Tet family participates in the physiological response to ischemia. Our study shows that hypercholesterolemia specifically decreases the expression of Tet1 in HSCs (Supplementary Fig 3). The chimeric WT mice reconstituted with Tet1$^{-/-}$ HSCs showed a significant reduction in blood flow recovery, collateral artery diameter, and capillary density after the induction of hindlimb ischemia (Fig 3, *A-C* and *E*).

Tet proteins also participate in the regulation of histone modifications. The O-linked N-acetylglucosamine transferase, OGT, is an evolutionarily conserved enzyme that catalyzes O-linked protein glycosylation. Tet proteins were identified as stable partners of OGT in the nucleus.[38,39] The interaction of Tet2 and Tet3 with OGT leads to the GlcNAcylation of host cell factor 1 that contributes to the integrity of the H3K4 methyltransferase SET1/COMPASS complex, revealing that Tet proteins increase the level of H3K4me3, a modification that functions in transcriptional activation.[40] Our previous study showed that OGT also interacts with Tet1 in HSCs.[28] Consistent with these findings, we found a decrease in the H3K4me3 modification near the promoters of all the genes we investigated (Fig 6). These results suggest that Tet1 regulates the expression of genes related to the differentiation of Ly6C^{low} monocytes by multiple epigenetic mechanisms.

We have previously shown that Tet1 expression in HSCs also regulates their differentiation toward NKT and γδ T cells and that the effects of hypercholesterolemia on colorectal tumor incidence are mediated by the downregulation of Tet1 in HSCs.[28] We now show that Tet1 expression also regulates HSC differentiation toward the monocyte subsets. In further support of this novel mechanism in which immune cell gene expression is regulated by epigenetic reprogramming within the HSCs, we also showed that type 2 diabetes mellitus impairs wound healing through an HSC autonomous mechanism that is driven by a Nox 2-dependent increase in HSC oxidant stress that increased Dnmt1, which, in turn, reduced the concentration of macrophages during the early phases of wound healing and skewed their polarization to M1 inflammatory macrophages.[41] Together, these results show a novel mechanism by which the gene expression of innate immune and naive T cells are regulated by oxidant stress-dependent HSC autonomous epigenetic mechanisms.

The clinical implications of this study are potentially significant. The current management of intermittent claudication has become unsettled.[42-45] After 5 to 8 years of follow-up, revascularization strategies for intermittent claudication lose their early benefits and do not result in any long-term improvement in health-related quality of life or walking capacity compared with a noninvasive strategy.[42,43] Moreover, revascularization resulted in an increased rate of progression to chronic limb-threatening ischemia and an increased amputation rate.[44] We show that the immune cell response, principally the monocyte subsets, is the dominant mechanism regulating collateral artery enlargement. There is still no highly efficacious drug or cell therapy to increase collateral artery blood flow. The results of this study provide a new framework for developing effective drug or cell therapies that restore Tet1 expression in hematopoietic stem cells.

An important limitation of this study is that we did not explore gender differences, which might be significant. Similarly, functional studies such as Tarlov scale would have added to the clinical significance of the work. Finally, we did not measure any serum markers of inflammation.

AUTHOR CONTRIBUTIONS

DISCLOSURES

None.

REFERENCES

1. Ganta VC, Choi MH, Kutateladze A, Fox TE, Farber CR, Annex BH. A MicroRNA93-interferon regulatory factor-9-immunoresponsive gene-1-itaconic acid pathway modulates M2-like macrophage polarization to revascularize ischemic muscle. *Circulation*. 2017;135:2403—2425.

2. Seiler C. The human coronary collateral circulation. *Eur J Clin Invest*. 2010;40:465–476.

3. Wang S, Zhang H, Dai X, Sealock R, Faber JE. Genetic architecture underlying variation in extent and remodeling of the collateral circulation. *Circ Res*. 2010;107:558–568.

4. Ebrahimian TG, Heymes C, You D, et al. NADPH oxidase-derived overproduction of reactive oxygen species impairs postischemic neovascularization in mice with type 1 diabetes. *Am J Pathol*. 2006;169:719–728.9.

5. Auffray C, Fogg D, Garfa M, et al. Monitoring of blood vessels and tissues by a population of monocytes with patrolling behavior. *Science*. 2007;317:666–670.

6. Carlin LM, Stamatiades EG, Auffray C, Hanna RN, Glover L, Vizcay-Barrena G. Nr4a1-dependent Ly6C(low) monocytes monitor endothelial cells and orchestrate their disposal. *Cell*. 2013;153:362–375.

7. Jetten N, Donners MM, Wagenaar A, et al. Local delivery of polarized macrophages improves reperfusion recovery in a mouse hind limb ischemia model. *PLoS One*. 2013;8:e68811.

8. Capoccia BJ, Gregory AD, Link DC. Recruitment of the inflammatory subset of monocytes to sites of ischemia induces angiogenesis in a monocyte chemoattractant protein-1-dependent fashion. *J Leukoc Biol*. 2008;84:760–768.

9. Silvestre JS, Smadja DM, Levy BI. Postischemic revascularization: from cellular and molecular mechanisms to clinical applications. *Physiol Rev*. 2013;93:1743–1802.

10. Chu HX, Broughton BR, Kim HA, Lee S, Drummond GR, Sobey CG. Evidence that Ly6C(hi) monocytes are protective in acute ischemic stroke by promoting M2 macrophage polarization. *Stroke*. 2015;46: 1929–1937.

11. Cochain C, Rodero MP, Vilar J, et al. Regulation of monocyte subset systemic levels by distinct chemokine receptors controls post-ischaemic neovascularization. *Cardiovasc Res*. 2010;88:186–195.

12. Guilliams M, Mildner A, Yona S. Developmental and functional heterogeneity of monocytes. *Immunity*. 2018;49:595–613.

13. van der Laan AM, Hirsch A, Robbers LF, et al. A proinflammatory monocyte response is associated with myocardial injury and impaired functional outcome in patients with ST-segment elevation myocardial infarction: monocytes and myocardial infarction. *Am Heart J*. 2012;163:57–65.e2.

14. Honold L, Nahrendorf M. Resident and monocyte-derived macrophages in cardiovascular disease. *Circ Res*. 2018;122:113–127.

15. Fogg DK, Sibon C, Miled C, et al. A clonogenic bone marrow progenitor specific for macrophages and dendritic cells. *Science*. 2006;311:83–87.

16. Hettinger J, Richards DM, Hansson J, et al. Origin of monocytes and macrophages in a committed progenitor. *Nat Immunol*. 2013;14:821–830.

17. Ginhoux F, Jung S. Monocytes and macrophages: developmental pathways and tissue homeostasis. *Nat Rev Immunol*. 2014;14:392–404.

18. Gamrekelashvili J, Giagnorio R, Jussofie J, et al. Regulation of monocyte cell fate by blood vessels mediated by Notch signalling. *Nat Commun*. 2016;7:12597.

19. Avraham-Davidi I, Yona S, Grunewald M, et al. On-site education of VEGF-recruited monocytes improves their performance as angiogenic and arteriogenic accessory cells. *J Exp Med*. 2013;210:2611–2625.

20. Klug M, Schmidhofer S, Gebhard C, Andreesen R, Rehli M. 5-Hydroxymethylcytosine is an essential intermediate of active DNA demethylation processes in primary human monocytes. *Genome Biol*. 2013;14:R46.

21. Hirsch AT, Hartman L, Town RJ, Virnig BA. National health care costs of peripheral arterial disease in the Medicare population. *Vasc Med*. 2008;13:209–215.

22. Babu M, Durga Devi T, Makinen P, et al. Differential promoter methylation of macrophage genes is associated with impaired vascular growth in ischemic muscles of hyperlipidemic and type 2 diabetic mice: genome-wide promoter methylation study. *Circ Res*. 2015;117:289–299.

23. Faggiano P, Pirillo A, Griffo R, et al. Prevalence and management of familial hypercholesterolemia in patients with coronary artery disease: the heredity survey. *Int J Cardiol*. 2018;252:193–198.

24. Perez de Isla L, Alonso R, Mata N, et al. Insights from the SAFEHEART registry (Spanish familial hypercholesterolaemia cohort study). *Arterioscler Thromb Vasc Biol*. 2016;36:2004–2010.

25. Lloyd-Jones D, Adams R, Carnethon M, et al. American Heart association statistics C and stroke statistics S. Heart disease and stroke statistics–2009 update: a report from the American Heart association statistics committee and stroke statistics subcommittee. *Circulation*. 2009;119:480–486.

26. van Weel V, de Vries M, Voshol PJ, et al. Hypercholesterolemia reduces collateral artery growth more dominantly than hyperglycemia or insulin resistance in mice. *Arterioscler Thromb Vasc Biol*. 2006;26: 1383–1390.

27. Tirziu D, Moodie KL, Zhuang ZW, et al. Delayed arteriogenesis in hypercholesterolemic mice. *Circulation*. 2005;112:2501–2509.

28. Tie G, Yan J, Khair L, et al. Hypercholesterolemia increases colorectal cancer incidence by reducing production of NKT and gammadelta T cells from hematopoietic stem cells. *Cancer Res*. 2017;77:2351–2362.

29. Pastor WA, Aravind L, Rao A. TETonic shift: biological roles of TET proteins in DNA demethylation and transcription. *Nat Rev Mol Cell Biol*. 2013;14:341–356.

30. Chambers SM, Boles NC, Lin KY, et al. Hematopoietic fingerprints: an expression database of stem cells and their progeny. *Cell Stem Cell*. 2007;1:578–591.

31. Zhang X, Zhang Y, Wang C, Wang X. TET (Ten-eleven translocation) family proteins: structure, biological functions and applications. *Signal Transduct Target Ther*. 2023 Aug 11;8:297.

32. Yan R, Cheng X, Gu C, et al. Dynamics of DNA hydroxymethylation and methylation during mouse embryonic and germline development. *Nat Genet*. 2023;55:130–143.

33. Yan J, Tie G, Messina LM. Tetrahydrobiopterin, L-arginine and vitamin C act synergistically to decrease oxidative stress, increase nitric oxide and improve blood flow after induction of hindlimb ischemia in the rat. *Mol Med*. 2012;18:676–684.

34. Park B, Hoffman A, Yang Y, et al. Endothelial nitric oxide synthase affects both early and late collateral arterial adaptation and blood flow recovery after induction of hind limb ischemia in mice. *J Vasc Surg*. 2010;51:165–173.

35. Tie G, Messina KE, Yan J, Messina JA, Messina LM. Hypercholesterolemia induces oxidant stress that accelerates the ageing of hematopoietic stem cells. *J Am Heart Assoc*. 2014;3:e000241.

36. Taoudi S, Morrison AM, Inoue H, Gribi R, Ure J, et al. Progressive divergence of definitive haematopoietic stem cells from the endothelial compartment does not depend on contact with the foetal liver. *Development*. 2005 Sep;132:4179–4191.

37. Huang N, Tan L, Xue Z, Cang J, Wang H. Reduction of DNA hydroxymethylation in the mouse kidney insulted by ischemia reperfusion. *Biochem Biophys Res Commun*. 2012;422:697–702.

38. Vella P, Scelfo A, Jammula S, et al. Tet proteins connect the O-linked N-acetylglucosamine transferase Ogt to chromatin in embryonic stem cells. *Mol Cell*. 2013;49:645–656.

39. Shi FT, Kim H, Lu W, et al. Ten-eleven translocation 1 (Tet1) is regulated by O-linked N-acetylglucosamine transferase (Ogt) for target gene repression in mouse embryonic stem cells. *J Biol Chem*. 2013;288:20776–20784.

40. Deplus R, Delatte B, Schwinn MK, et al. TET2 and TET3 regulate GlcNAcylation and H3K4 methylation through OGT and SET1/COMPASS. *EMBO J*. 2013;32:645–655.

41. Yan J, Tie G, Wang S, et al. Diabetes impairs wound healing by Dnmt1-dependent dysregulation of hematopoietic stem cells differentiation towards macrophages. *Nat Commun*. 2018;9:33.

42. Djerf H, Millinger J, Falkenberg M, Jivegård L, Svensson M, Nordanstig J. Absence of long-term benefit of revascularization in patients with intermittent claudication: five-year results from the IRONIC randomized controlled trial. *Circ Cardiovasc Interv*. 2020;13: e008450.

43. Gunnarsson T, Gottsäter A, Bergman S, Troëng T, Lindgren H. Eight-year outcome after invasive treatment of infrainguinal intermittent claudication: a population-based analysis from the Swedish vascular register (Swedvasc). *SAGE Open Med*. 2020;8:2050312120926782.

44. Madabhushi V, Davenport D, Jones S, Khoudoud SA, Orr N, et al. Revascularization of intermittent claudicants leads to more chronic limb-threatening ischemia and higher amputation rates. *J Vasc Surg*. 2021;74:771–779.

45. McCready RA, Brown OW, Kiell CS, Goodson SF. Revascularization for claudication: changing the natural history of a benign disease!. *J Vasc Surg*. 2023 Aug 22;79:159–166.